Theoretical Notes
Note 193

SLA-73-0494

ELECTRON ATTACHMENT AND AVALANCHING ASSOCIATED WITH EMP CALCULATIONS FOR HIGH-ALTITUDE BURSTS

Charles N. Vittitoe

Theoretical Division
Simulation Sciences Research Department
Sandia Laboratories
Albuquerque, New Mexico
87115

A presentation at the DNA EMP Phenomenology Working Group (EMPPWOG) meeting at the Air Force Weapons Laboratory, Kirtland Air Force Base, Albuquerque, New Mexico, May 3-4, 1973

Abstract

The electron attachment and avalanching parameters currently in the SHARP code have been collected in a form which should facilitate comparison with parameters used in other codes. The method of obtaining the necessary data and the conversion for EMP codes are discussed. A limited comparison is made between the representations in SHARP and those in use elsewhere.

TABLE OF CONTENTS

	Page
Introduction	3
Avalanching and Two-body Attachment Data	4
Extension to Higher and Lower Field Values	7
The Electron Mobility	11
Three-body Attachment	13
Recapitulation	19
More Comparison with other Representations	20
A Recommendation	23

ELECTRON ATTACHMENT AND AVALANCHING ASSOCIATED WITH EMP CALCULATIONS FOR HIGH-ALTITUDE BURSTS

Introduction

The electron attachment and avalanching parameters presently in the SHARP (Sandia High Altitude Radioflash Prediction) code have been in use in the present form for about two years. Since the code is designed for high-altitude bursts and for time spans up to 500 nsec, many electron processes are justifiably neglected. More of these interactions should be taken into account if the code is extended to later times.

The attachment and avalanching parameters are required in EMP codes in order to calculate the secondary electron number density and subsequently the air conductivity for substitution into Maxwell's equations. The time rate of change of the secondary electron number density is

$$\dot{\eta}_{sec} = \dot{\eta} + (\alpha_i - \alpha_a)\, \mu\, E\, \eta_{sec} \quad , \tag{1}$$

where

$\alpha_i \equiv$ Townsend avalanche (ionization) coefficient,

$\alpha_a \equiv$ attachment coefficient,

$\mu \equiv$ electron mobility,

$E \equiv$ electric field intensity,

and where $\dot{\eta}$ is the rate of secondary electron production caused by the Compton electrons slowing down and associated processes such as secondary

electron thermalization. Data are usually reported for the parameters α_i, α_a, and μ as a function of E, and possibly as a function of air density (ρ), air pressure (p), or as a function of the molecular number density (N). Thus rate coefficients for avalanching ($\alpha_i \mu E$) and for attachment ($\alpha_a \mu E$) must be formulated for Eq. (1) in EMP codes. An additional complication occurs because the attachment-rate coefficient is the net result of several chemical reactions. Some of these reactions involve two "bodies" with a rate proportional to the air density. Other reactions involve three "bodies" and have a rate proportional to the square of the air density. With the rate-coefficient for two-body effects denoted by $\alpha_{a1}\rho/\rho_o$ and that for three-body effects denoted by $\alpha_{a2}(\rho/\rho_o)^2$,

$$\alpha_a \mu E = \alpha_{a1} + \alpha_{a2}\, \rho/\rho_o = \beta\, \rho_o/\rho$$

where ρ_o is the reference sea-level air density and β is the actual rate coefficient.

Avalanching and Two-body Attachment Data

The electron attachment and ionization parameters used in the SHARP code are the result of several compromises. The basic source from which these parameters were obtained is a compilation of such data by Phelps in 1967.[1] The essential data are given in Fig. 1. A series of α_i/N and α_{a1}/N values read from Phelps' graphs are listed in Table I. At E/N near 6×10^{-16} V - cm^2, the spread in the experimental data for two-body attachment is so large that Phelps recommended using the theoretical

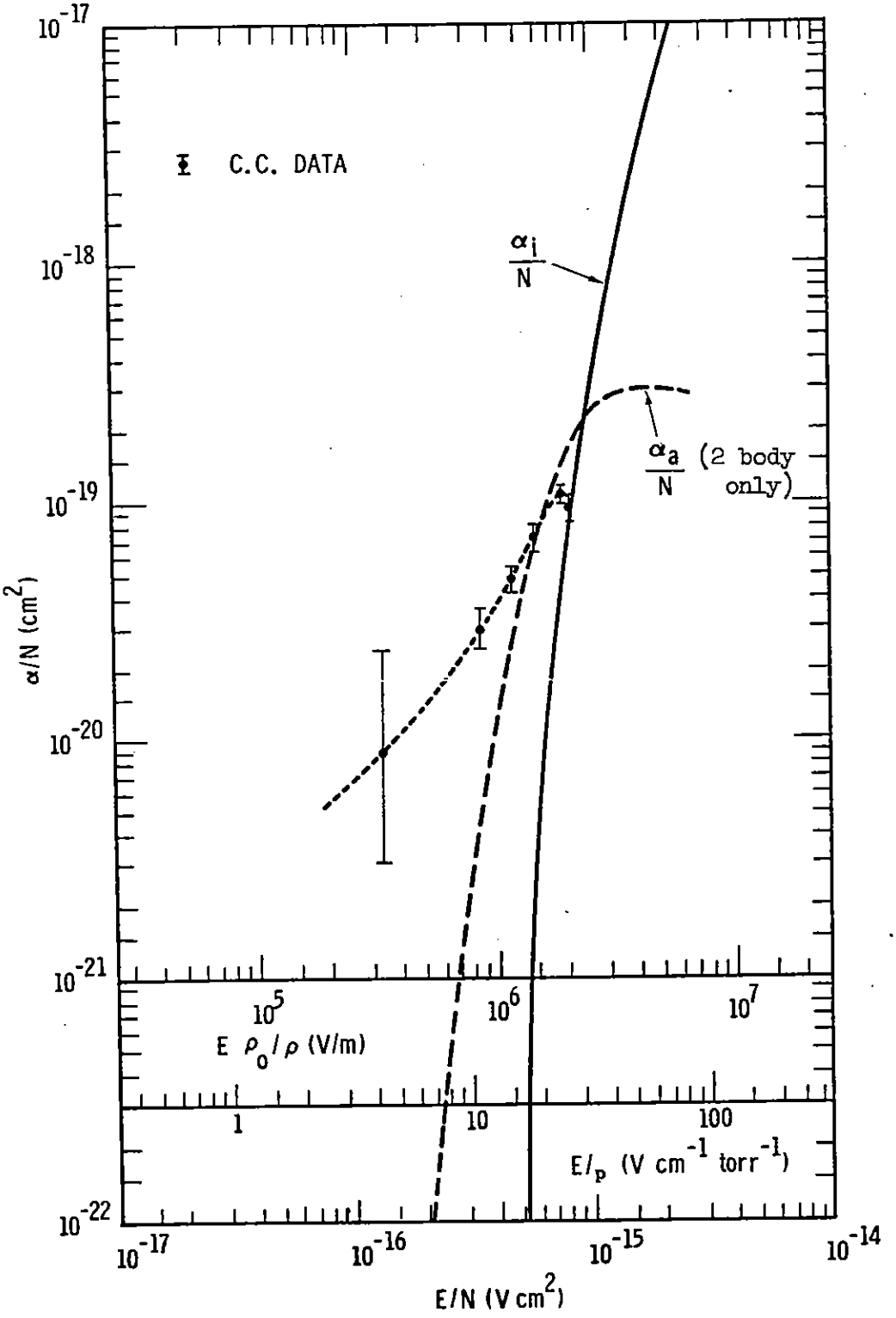

Fig. 1 - Attachment and ionization coefficients versus E/N for air

Table I. A portion of the data obtained from A. V. Phelps' graph

E/N	α_i/N	α_a/N	EN_o/N	EN_o/N	$\alpha_i N_o/N$	$\alpha_a N_o/N$	$\mu N/N_o$	$\alpha_i \mu EN_o/N$	$\alpha_a \mu EN_o/N$
10^{-16} V cm^2	10^{-21} cm^2	10^{-20} cm^2	10^5 V/m	esu	cm^{-1}	cm^{-1}	10^{-2} m^2/Vsec	10^5 sec^{-1}	10^5 sec^{-1}
2.1	--------	0.012	5.2	17.3	----------	0.003	7.4	--------	0.12
2.5	--------	0.056	6.2	20.7	----------	0.014	7.1	--------	0.62
3.0	--------	0.21	7.5	25.0	----------	0.052	6.7	--------	2.61
3.5	--------	0.54	8.8	29.3	----------	0.14	6.4	--------	7.88
4.0	--------	1.12	10.0	33.3	----------	0.28	6.2	--------	17.4
5.0	--------	3.20	12.5	41.7	----------	0.80	6.1	--------	61.0
5.2	0.1	3.70	13.0	43.3	2.5(-3)[a]	0.92	6.0	0.2	71.8
6.0	4.0	7.4	15.0	50.0	1.0(-1)	1.85	5.9	8.8	164.
6.6	14.0	10.3	16.5	55.0	3.5(-1)	2.58	5.7	32.9	243.
7.0	24.0	12.0	17.5	58.3	6.0(-1)	3.00	5.5	57.8	289.
8.0	60.0	16.5	20.0	66.7	1.5	4.12	5.4	162.	445.
9.0	150.0	19.5	22.5	75.0	3.8	4.88	5.2	445.	571.
10.0	280.	23.0	25.0	83.3	7.0	5.75	4.9	858.	704.
11.0	470.	25.0	27.5	91.7	11.8	6.25	4.6	1490.	791.
12.0	750.	26.8	30.0	100.0	18.8	6.70	4.5	2540.	904.
13.0	1100.	27.8	32.5	108.3	27.5	6.95	4.4	3930.	994.
14.0	1500.	28.4	35.0	116.7	35.7	7.10	4.4	5.5(3)	1090.
15.0	2000.	28.6	37.5	125.0	50.0	7.15	4.3	8.1(3)	1150.
16.0	2600.	29.0	40.0	133.3	65.0	7.25	4.3	1.1(4)	1250.
17.0	3300.	29.1	42.5	141.7	82.5	7.28	4.3	1.5(4)	1330.
18.0	4300.	29.1	45.0	150.0	107.5	7.28	4.2	2.0(4)	1380.
19.0	5300.	29.1	47.5	158.3	132.5	7.28	4.2	2.6(4)	1450.
20.0	6100.	29.1	50.0	166.7	152.5	7.28	4.2	3.2(4)	1530.
21.0	7000.	29.1	52.5	175.0	175.0	7.28	4.1	3.8(4)	1570.
22.0	8200.	29.0	55.0	183.3	205.0	7.25	4.1	4.6(4)	1630.
23.0	10000.	28.7	57.5	191.7	250.0	7.18	4.0	5.8(4)	1650.
24.0	--------	28.5	60.0	200.0	----------	7.12	4.0	---------	1710.
25.0	--------	28.2	62.5	208.3	----------	7.05	3.9	---------	1720.

$N_o = 2.5 \times 10^{19}$ cm^{-3} (air at 1 atmosphere pressure and 20° C).

$\mu N/N_o$ obtained from graph of analytic fit.

a indicates 2.5×10^{-3}

curve given in Fig. 1 for α_a/N until the experimental situation is clarified.[1] The molecular number density at sea level, $N_o = 2.5 \times 10^{19}$ molecules/cm^3, is used to generate the additional horizontal scales in Fig. 1.

The C. C. (Chatterton-Craggs) data[2] in Fig. 1 give an indication of the effect of three-body interactions. These data were taken at 5.9 to 17.4 torr and 288 K. They are in sharp contrast to data taken for oxygen alone, where in this pressure range three-body processes are significant only for $E/p_{O_2} < 4$V cm^{-1} torr^{-1}.[3] For the same O_2 pressure to be present, the corresponding E/p_{air} is about 0.8 V cm^{-1} torr^{-1}. The C. C. data indicate three-body processes are significant in air for E/p < 15 V cm^{-1} torr^{-1}.

Extension to Higher and Lower Field Values

As the value of E/p increases beyond 40 V cm^{-1} torr^{-1}, data become scarce. In this region the ionization coefficient is several orders of magnitude above the two-body attachment coefficient. Hence attachment can be neglected. For E/p between 10 and 10^3V cm^{-1} torr^{-1}, Kontaratos[4] suggested the following equation to describe variation of the first Townsend coefficient for dry air:

$$\frac{\alpha_i}{p} = 0.57 \exp\left[\frac{-222}{E/p}\right] \left\{\frac{(E/p)^{\frac{1}{2}}}{1+4\times10^{-4}E/p}\right\} \text{ cm}^{-1} \text{ torr}^{-1} \qquad (2)$$

where E/p is in V cm^{-1} torr^{-1}. Let $y = E\,\rho_o/\rho$ in esu. Then

$$y(\text{esu}) = 2.53\ E/p\ (\text{V cm}^{-1}\ \text{torr}^{-1}) \quad ,$$

and with

$$\frac{\rho}{\rho_o} = \frac{p}{p_o} \tag{3}$$

Eq. (2) becomes

$$\frac{\alpha_i \rho_o}{\rho} = 272 \exp\left[-\frac{561.6}{y}\right]\left\{\frac{\sqrt{y}}{1+1.58\times10^{-4}y}\right\} \text{cm}^{-1} \quad . \tag{4}$$

Eq. (4) is useful over the range

$$25.3 < y \leq 2530 \text{ esu} \quad . \tag{5}$$

For $y > 2530$ esu, the form suggested by Arnush,[5] et al., is

$$\frac{\alpha_i}{p} = 13 - 505\left(\frac{E}{p}\right)^{-0.8} \quad , \tag{6}$$

or

$$\frac{\alpha_i \rho_o}{\rho} = 9880. - 8.06 \times 10^5 (y)^{-0.8} \text{ cm}^{-1} \tag{7}$$

As Arnush, et al., point out,[5] this higher field region is difficult to represent with high reliability.

The low y regions also involve uncertainties. The C. C. data go to $E/p \approx 6$ V cm^{-1} torr^{-1} for attachment of electrons in air. At lower y values, data are available for individual gases such as O_2 and N_2, but not for air. Longmire and Malik[6] have combined these N_2, O_2 data into attachment rate estimates for air:

$$\beta(10^8 \text{sec}^{-1}) = \left\{\frac{1.1 + 14y}{1. + 22y^{1.44}} - 0.04\right\}\left(\frac{\rho}{\rho_o}\right)^2 + \left\{\frac{1.9 \times 10^{-7} y^5}{1. + 1.5 \times 10^{-8} y^6}\right\}\left(\frac{\rho}{\rho_o}\right) \tag{8}$$

A different version of this variation as used in the CHAP program[7] is

$$\beta(\text{sec}^{-1}) = \frac{6.3 \times 10^7}{\sqrt{y + 0.1}}\left(\frac{\rho}{\rho_o}\right)^2 + 1.3 \times 10^8 \frac{\rho}{\rho_o} \exp\left[\frac{-100\ \rho/\rho_o}{E + 10^{-4}}\right],$$

where E and y are in esu. For $\rho = \rho_o$ Fig. 2 gives a comparison of these functions with those in SHARP with the two- and three-body terms separated. The criticism might be raised that the electron mobility and attachment rates are usually obtained from steady-state types of experiments, and, hence, the constituents of the air may be altered from those in the atmosphere. Thus, parameters obtained by combining N_2 and O_2 data would be more appropriate than results measured for air, since the EMP is too fast for the composition to change to that in the steady-state experiments. However, the experiments add extremely small amounts of energy to the medium, so there is little possibility of change in the composition of air.[8] Typical currents in such experiments are on the order of 10^{-10} amperes.[8]

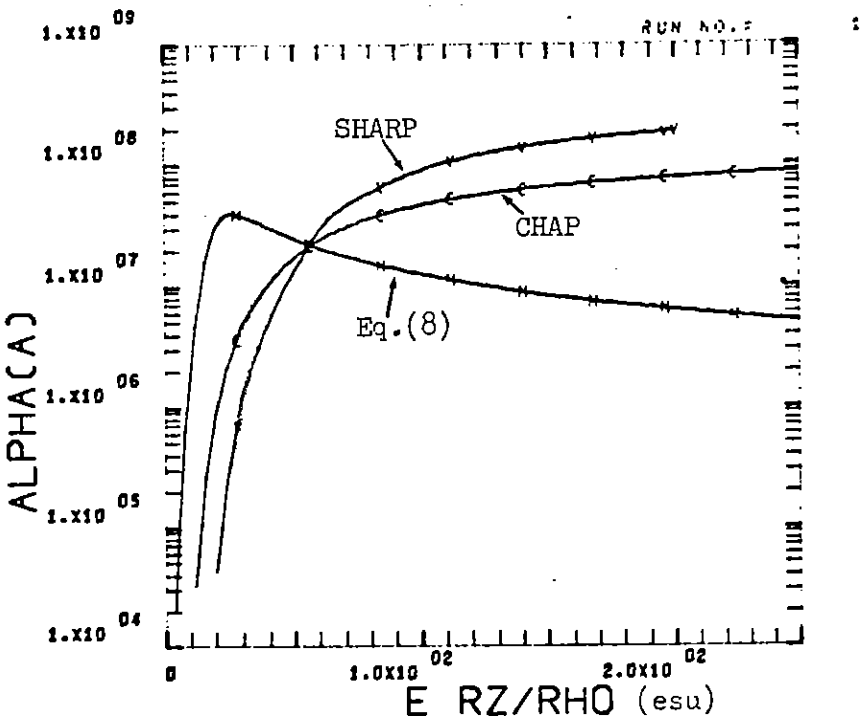

Fig. 2a. A comparison of the two-body attachment rate ($\alpha_{a1}\rho_o/\rho$) in Eq. (8) with those used in CHAP and in SHARP.

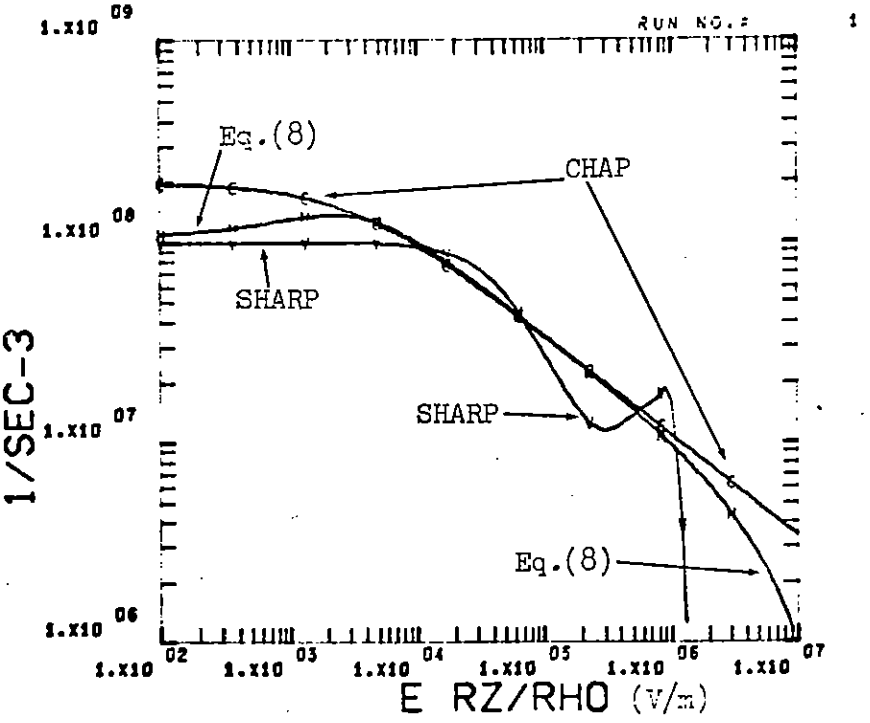

Fig. 2b. A comparison of the three-body attachment rate ($\alpha_{a2}\rho_o^2/\rho^2$) in Eq. (8) with those used in CHAP and in SHARP.

The Electron Mobility

The variation of electron mobility with electric field strength and atmospheric density used by SHARP is given by the rational function approximation

$$\frac{\mu\rho}{\rho_o} = \frac{1.62 + \sum_{i=1}^{4} A_i (E\rho_o/\rho)^i}{1. + \sum_{i=1}^{5} B_i (E\,\rho_o/\rho)^i} \quad , \tag{11}$$

with

$A_1 = 1.1321417712\ 10^{-5}$ $\qquad$ $B_1 = 1.8499033641\ 10^{-4}$

$A_2 = -\ 6.4273213607\ 10^{-12}$ $\qquad$ $B_2 = -\ 6.5335355782\ 10^{-11}$

$A_3 = 6.0323166013\ 10^{-19}$ $\qquad$ $B_3 = -\ 1.1862042487\ 10^{-17}$

$A_4 = 5.0549330598\ 10^{-26}$ $\qquad$ $B_4 = 4.0923235457\ 10^{-24}$

$B_5 = -\ 8.2445039013\ 10^{-32}$

when E is in V/m and μ is in $m^2/(V\ sec)$. This approximation is reasonable in the region

$$0 \le E\,\rho_o/\rho \le 10^6 \text{ V/m} \quad .$$

For larger values the variation assumed is

$$\mu\,\rho_o/\rho = \frac{2.024}{\sqrt[4]{E\,\rho_o/\rho}} \quad , \tag{12}$$

with a lower bound of $2.17 \times 10^{-2}\ m^2V^{-1}\ sec^{-1}$. Such a break is necessary because of a discontinuity in the rational function near 2×10^6 V/m, as indicated in Fig. 3. As noted in Fig. 3, data points for the fit

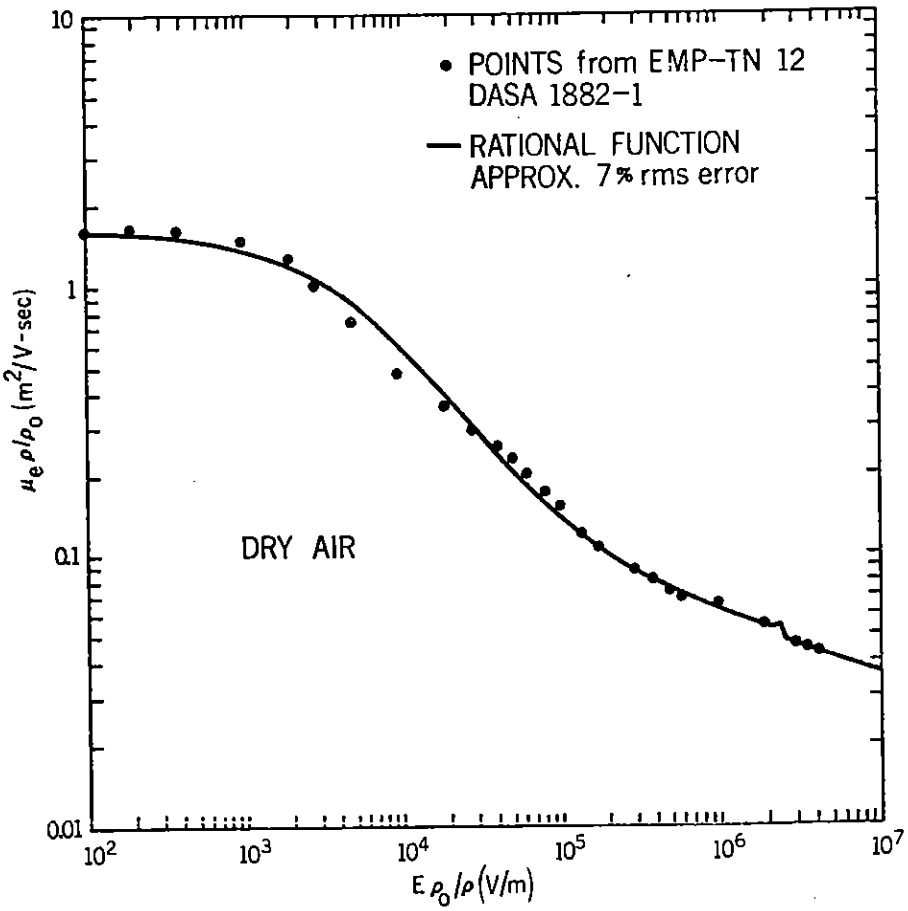

Fig. 3. Electron mobility in air vs. applied field intensity.

were obtained from Carl Baum's 1965 article.[9] If this fit were to be repeated now, it is likely that critical review would alter the choice of data somewhat. A spline curve-fitting procedure would also be used. However, it is not clear that the present data justify a fit with better than the 7% rms error noted in Fig. 3. A. V. Phelps indicated[1] that at high E/N the mobility is likely to increase with increasing E/N. He suggested the increase may be associated with greater forward scattering and a reduction in the $\langle 1 - \cos\theta \rangle$ factor which enters the momentum transfer cross section. Such a minimum does occur in H_e and H_2 data near $E/N \sim 10^{-15}$ V cm^2 [1]. Thus, the mobility variation may be improved at a later date.

Three-body Attachment

Inconsistencies occur when comparing the various sources of avalanching and attachment coefficients. Concentration on attachment rates for three-body effects in air yields Fig. 4. The solid curve is the spline fit used by SHARP. The hump near 10^6 V/m is suspected not to be real.[8] The three-body attachment curve is expected to continue downward with a slope similar to its value at 10^5 V/m. In most high-altitude burst situations, the air density is sufficiently low that three-body attachment gives only a slight effect, so the hump should not influence the results significantly. Neglect of the hump also requires justification of neglect of the 100 and 200 torr data points which appear to agree quite well with each other near 8×10^5 V/m. The most reliable three-body attachment data for air appear to be those of Hessenauer[10] that are listed in Table II. Other data by Chatterton and Craggs[2] and by Kuffel[11] only indicate the pressure ranges at which data were taken. For example, Kuffel[11] noted that his data were recorded in the range $6.8 \leq p \leq 10.0$ mm Hg. The pressure corresponding to specific data points was not reported. At the low-field limit, the 10^8 sec^{-1} attachment rate may be in error. Channin, et al., predict a value of 7×10^7 sec^{-1} at $N_o = 2.5 \times 10^{19}$ cm^{-3} and 300 K.[12] They report their value is lower than previous estimates. Judging from the data in Fig. 4, a theoretical curve could likely be used for three-body attachment also. A theory for these processes has not yet been developed.[8]

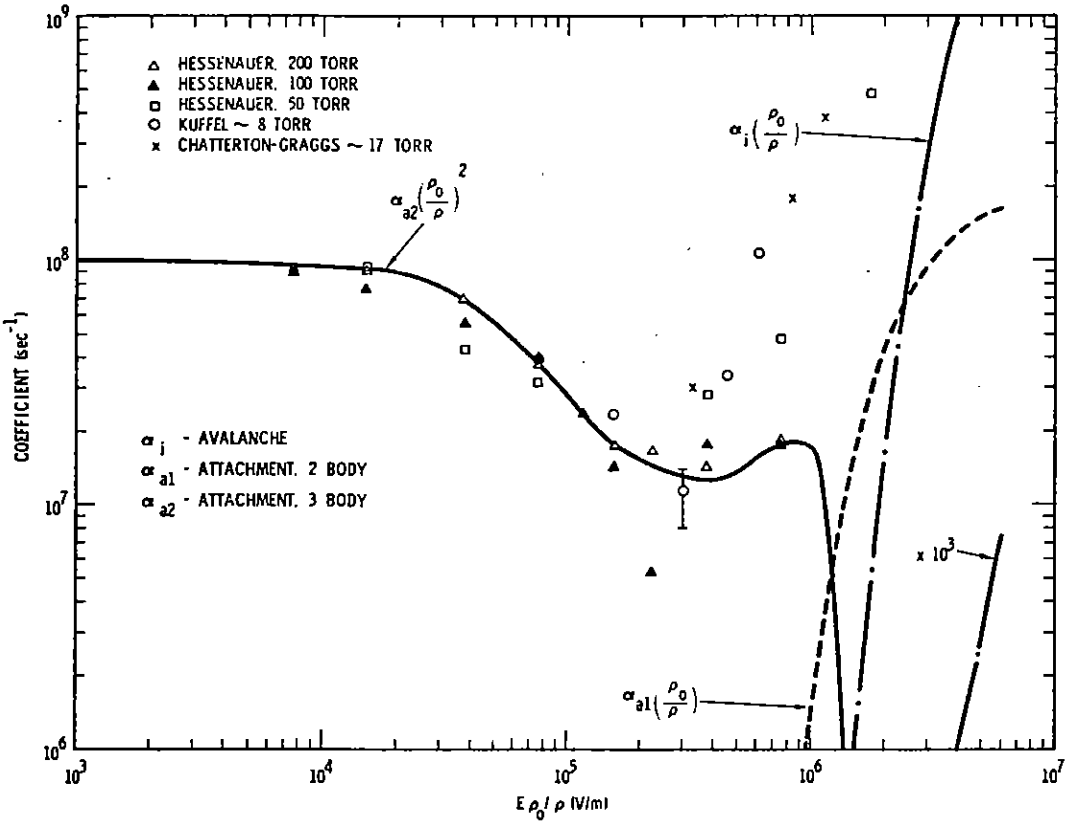

Fig. 4. Attachment and avalanche rates in air vs. normalized field intensity.

The spline fit of the avalanching data and the two- and three-body attachment data are illustrated in Fig. 5. The fits were generated by an early version of the UNFOLD[13] program, with help from Ruth Lighthill and Frank Biggs of Sandia Laboratories. The general form for a cubic spline is

$$f(z) = \delta_1 + \delta_2 z + \delta_3 z^2 + \delta_4 z^3 + \sum_{j=5}^{K} \delta_j (z - \gamma_j)_+^3 ,$$

where $(w)_+ = wh(w)$, and $h(w)$ is the Heaviside unit step function. The

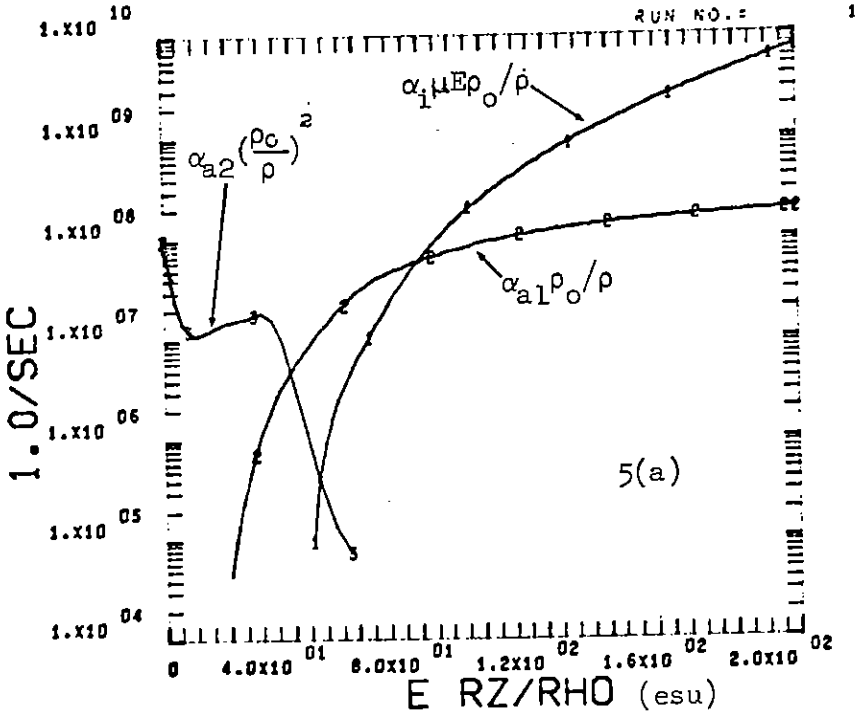

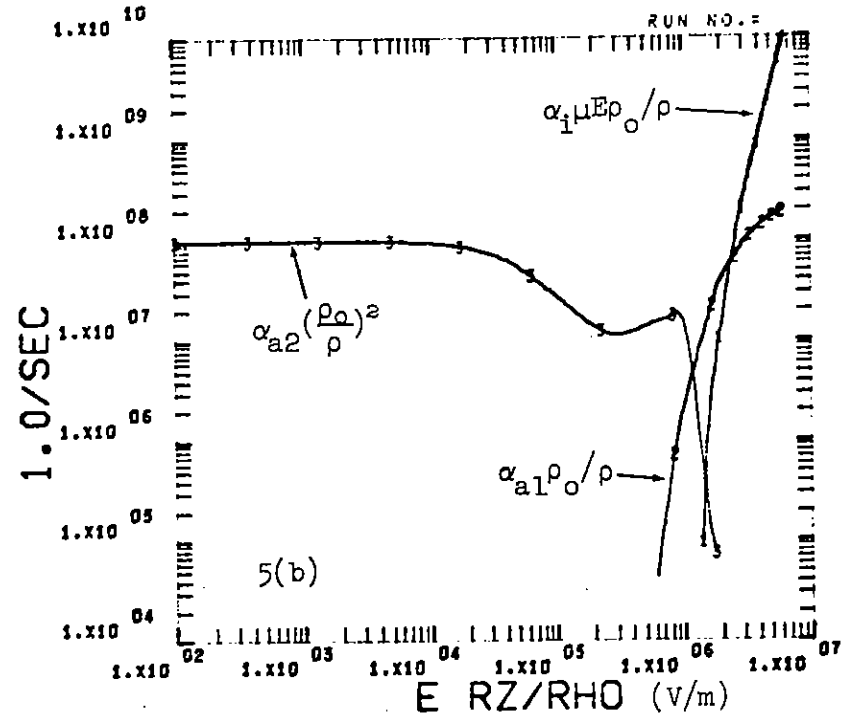

Fig. 5. Electron avalanching and attachment parameters.

Table II. Three-body-attachment Coefficient Data for Air

E/p V/(cm-torr)	$E\rho_o/\rho$ kV/m	Attachment Coefficient[11] $\frac{\beta}{\mu E}$ (cm^{-1}) p = 50 torr $N=1.65\times10^{18}\ cm^{-3}$	p = 100 torr $N=3.3\times10^{18}\ cm^{-3}$	p = 200 torr $N=6.6\times10^{18}\ cm^{-3}$	Drift Velocity $V_D = \mu E$ (10^6 cm/sec)
0.1	7.6		3.6	15	0.42
0.2	15.2	0.67	2.2	10.5	0.61
0.5	38.0	0.20	1.0	4.9	0.95
1.0	76.0	0.11	0.56	2.1	1.25
1.5	114.0		0.27	----	1.50
2.0	152.0		0.15	0.72	1.68
3.0	228.0		0.04	0.51	2.30
5.0	380.0	0.04	0.10	----	3.10
10.0	760.0	0.04	0.06	0.29	5.20
15.0	1140.0		0.05	0.25	7.10
20.0	1520.0		0.15		8.00
22.5	1710.0	0.2	0.40		9.60
25.0	1900.0		0.2		10.5
30.0	2280.0		0.2		12.0
35.0	2660.0				13.0

parameter z is a function of y ($y = E\ \rho_o/\rho$ in esu) that is convenient for the fit. Table III lists parameters for the three curves. Each function is represented only in the range given. Outside the range, the attachment is neglected while the avalanching is represented by another form. After f(z) is found, the attachment or ionization rate (sec^{-1}) is obtained by raising the base e (or 10.) to the exponent f(z) and then multiplying by the proper power of the air density ratio.

Table III. Fit Parameters

	Functions		
	$z = y$	$z = y$	$z = \log_{10} y$
	$f(z) = \ell n\,[\alpha_i \rho_o/\rho]$	$f(z) = \ell n\,[\alpha_{a1} \rho_o/\rho]$	$f(z) = \log_{10}\,[\alpha_{a2} \rho_o^2/\rho^2]$
Parameter	44 esu $\leq y \leq$ 200 esu	20 esu $\leq y \leq$ 200 esu	0 $\leq y \leq$ 60 esu
δ_1	-2.4872887793(1)	1.5914108145(+1)	8.0000000000(+0)
δ_2	7.9069485666(-1)	-1.6626307256(+0)	2.7932011026(-14)
δ_3	2.2095580635(-16)	1.0495311264(-1)	7.3445017261(-15)
δ_4	-5.2678739418(-18)	-1.7492185440(-3)	6.0056011180(-15)
δ_5	-1.3265274555(-2)	2.0464881885(-3)	-5.4872069272(-2)
δ_6	1.8477990009(-2)	5.8235366016(-5)	-4.2930076068(-1)
δ_7	-4.9472053746(-3)	-2.9771484267(-4)	1.0011432014(+0)
δ_8	-3.5523110653(-4)	-1.3132783631(-4)	1.8200397658(+0)
δ_9	1.5962072104(-4)	1.3194978470(-4)	-6.7367830986(+0)
δ_{10}	-1.1175221266(-4)	-5.8652945216(-5)	1.9396095453(+1)
δ_{11}	5.4597169105(-5)	1.6542339312(-6)	-2.0743355229(+2)
δ_{12}	-1.1767242330(-5)	-7.5405859589(-7)	4.0800941511(+2)
δ_{13}	-2.2581411067(-7)	-3.4150609628(-7)	0.0
γ_5	45.5	23.0	-1.23
γ_6	47.5	30.0	-0.4
γ_7	52.0	36.0	0.1
γ_8	64.0	52.0	0.6
γ_9	74.0	61.0	1.0
γ_{10}	84.0	73.0	1.3
γ_{11}	90.0	92.0	1.43
γ_{12}	110.0	120.0	1.55
γ_{13}	172.0	148.0	----

Recapitulation

For $y \leq 200$ esu, a spline fit to the Phelps recommendation and a fit to the three-body attachment data are used as estimates for the attachment and avalanche rates in air. The attachment data are separated into two- and three-body contributions, as indicated in Fig. 5. For $200 < y \leq 2530$ esu, Eq. (4) for $\alpha_i \rho_o/\rho$ is used, (after renormalization as explained below) with calculations of $\mu(y)$ required for evaluation of the attachment rate. For $y > 2530$ esu, Eq. (7) is used (again, after renormalization) for the Townsend coefficient. It is suspected that inclusion of avalanching limits y to less than 200 esu and the other representations will be unnecessary for most electromagnetic pulse applications.

The Eq. (4) requires renormalization for continuity at $y = 200$ esu. Here the Phelps' curve indicates avalanching dominates, and

$$\alpha_i \mu E \, \rho_o/\rho = 7.1 \times 10^9 \text{ sec}^{-1} \quad .$$

Eq. (4) leads to

$$\alpha_i \mu E \, \rho_o/\rho = 5.4 \times 10^{10} \text{ sec}^{-1} \quad .$$

Renormalization of Eq. (4) for continuity at y = 200 esu gives

$$\frac{\alpha_i \rho_o}{\rho} (cm^{-1}) = 358. \exp\left[\frac{-561.6}{y}\right] \frac{\sqrt{y}}{1. + 1.58 \times 10^{-4} y} \quad . \qquad (13)$$

Figure 4 indicates the limits of mobility data for air. For $y > 2530$, $E\rho_o/\rho > 7.59\ 10^7$ V/m and no mobility data are available. If $\mu = 0.0217$ $m^2 V^{-1} sec^{-1}$ is assumed, the renormalization of Eq. (6) to preserve continuity at y = 2530 esu gives

$$\alpha_i \frac{\rho_o}{\rho} (sec^{-1}) = 7.95 \times 10^8 y - 6.48 \times 10^{10} y^{0.2} \quad . \qquad (14)$$

More Comparisons with Other Representations

Conrad Longmire has combined avalanching data for N_2 and O_2 and found an analytic approximation for air, as indicated below.[7]

$$\alpha_i \rho_o/\rho = \frac{5.7 \times 10^8\ y_1^5}{1. + 0.3\ y_1^{2.5}} sec^{-1} \qquad (15)$$

where

$$y_1 = \frac{E\rho_o}{100\rho} esu \quad .$$

Comparisons of the Longmire avalanching curve with that used by SHARP are given in Fig. 6. Recall that at the lower end of field intensity in Fig. 6 Phelps indicated a wide spread in the available data; thus he recommended use of the theoretical curve.[1] A change in choice for the ionization coefficient would then affect the data for two-body attachment

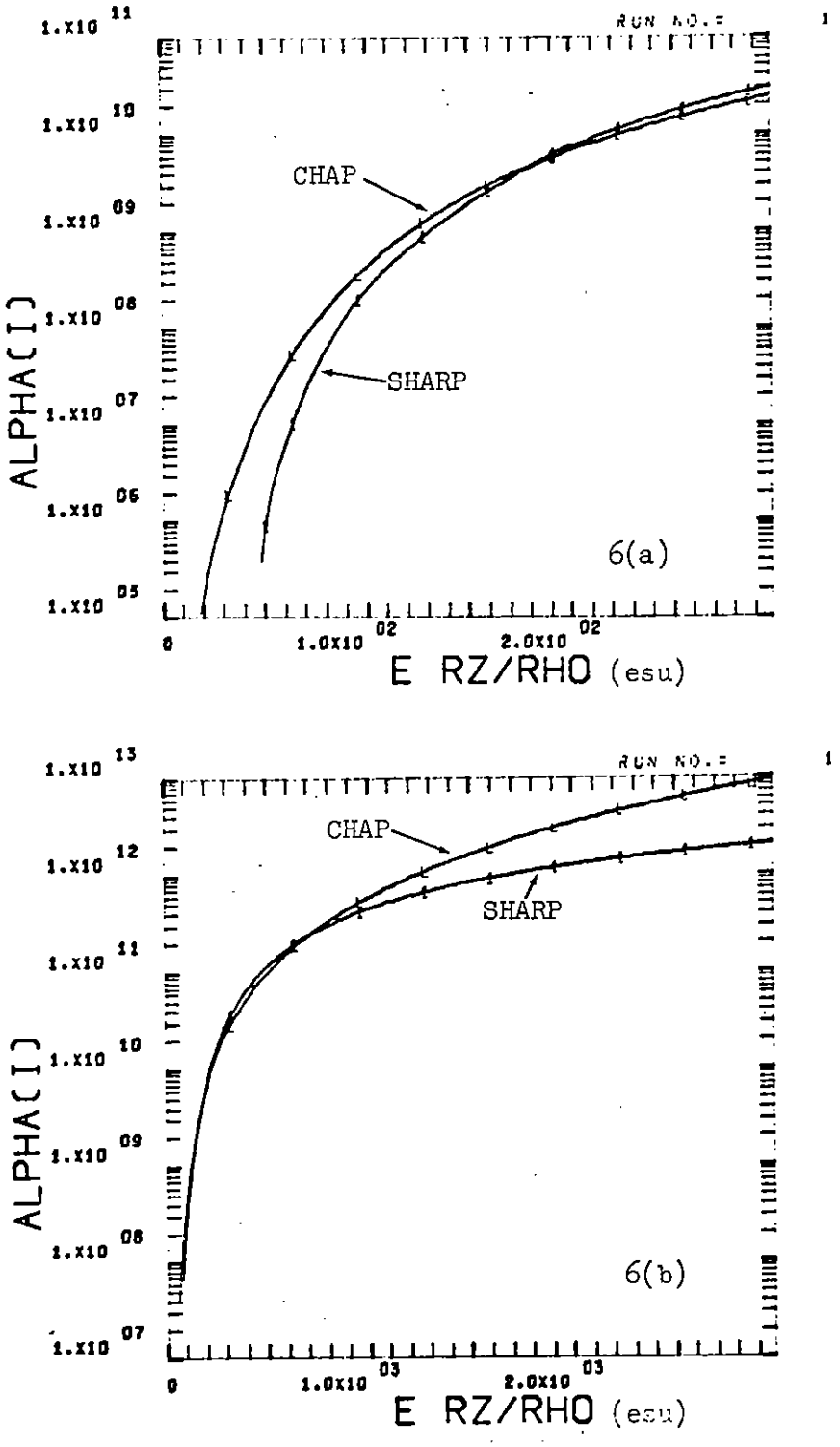

Fig. 6. Electron ionization rate, $\alpha_i \mu E \rho_o / \rho (sec^{-1})$ as a function of $E\rho_o/\rho$ as used in CHAP and SHARP.

in this $E\rho_o/\rho$ region. This may explain some of the differences that are illustrated in Fig. 2.

In the high altitude EMP code, NEPHI,[14] developed by the U. S. Army, the mobility is obtained from a five-piece curve fit.[14] The data Wyatt used for the fit were obtained from electron swarm measurements of the drift velocity. With E/p in V/(cm torr) and μ in $m^2\ V^{-1}\ sec^{-1}$, the equations are:

$$\frac{\mu\rho}{\rho_o} = \frac{2.092}{1. + 33.\ E/p}\ , \quad E/p \le 0.0303\ ;$$

$$\frac{\mu\rho}{\rho_o} = 1.809202 - 34.1606\ \frac{E}{p} + 332.685\left(\frac{E}{p}\right)^2 - 1186.94\left(\frac{E}{p}\right)^3\ ,$$

$$0.0303 < \frac{E}{p} \le 0.0905\ ;$$

$$\frac{\mu\rho}{\rho_o} = \frac{0.169267}{\sqrt{E/p}}\ , \quad 0.0905 \le \frac{E}{p} \le 0.4579\ ;$$

$$\frac{\mu\rho}{\rho_o} = 0.16212\ \exp\left\{0.04912\ \ell n^2\left(\frac{E}{p}\right) - 0.51686\ \ell n\left(\frac{E}{p}\right)\right\}, \quad 0.4579 < \frac{E}{p} \le 60;$$

$$\frac{\mu\rho}{\rho_o} = 0.033684 + \frac{0.6579}{(E/p)}\ , \quad 60. < \frac{E}{p}\ .$$

The CHAP code[7] uses the approximation $\mu\rho/\rho_o = 0.267\ \left\{\frac{6 + y^{0.85}}{1 + 6y^{0.85}}\right\}$ where μ is in $m^2/(V\ sec)$ and $y = E\rho_o/\rho$ (esu). Comparison of these representations with that used in SHARP is given in Fig. 7. Wyatt has also indicated[14] the attachment and ionization parameters used in NEPHI. Rather than give more detailed comparisons here, they will be left to the

EMPFWOG meeting. It is anticipated that more parameter fits will be presented there, so complete comparisons must wait till after digestion of the material presented at the meeting.

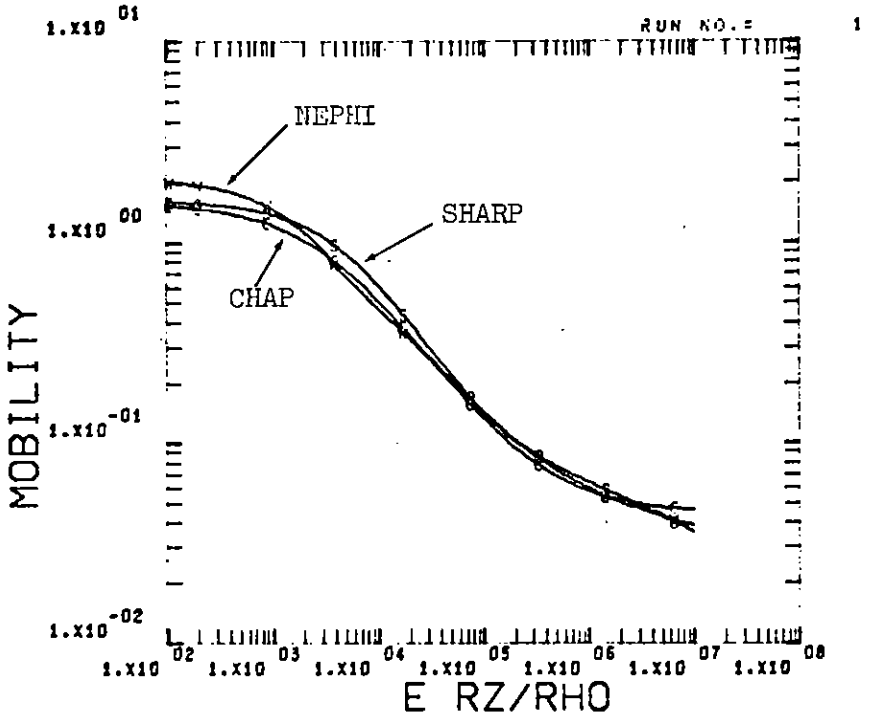

Fig. 7. Comparison of $\mu\rho/\rho_o(m^2V^{-1}sec^{-1})$ as a function of $E\rho_o/\rho(V/m)$ as represented in CHAP, NEPHI, and SHARP.

A Recommendation

There are other difficulties in the air parameters that have not yet been mentioned. For example, calculation of lower-altitude bursts must concern itself with the effect of water vapor. At least three sets of data are available for the 3% water vapor -- air mixture: those due to Phelps, Wyatt, and Baum.[15] At some values of $E\,\rho_o/\rho$, they differ by nearly 50 per cent.

The limited comparisons that have been made here illustrate one

main fact -- the spread in data is so large that various choices in data can give wide variations to the analytic representations of the parameters. This spread has been known for several years. It prompted a recommendation by Malik[15] and others more than three years ago. The need is still present. It is recommended that a molecular physicist review the air chemistry data and its representations, and attempt to produce a more reliable set. It is anticipated that further experiments will be required for such a parameter set to merit high confidence.

EMP calculators could probably agree to use the same analytic representations for the parameters. Such a step would be fine for comparison of codes. However, the expected improvement in the agreement between codes would not necessarily improve the reliability of the results.

References

1. Letters, A. V. Phelps to C. N. Vittitoe, February 20, 1970, and August 25, 1970.

2. P. A. Chatterton and J. D. Craggs, "Attachment Coefficient Measurements in Carbon Dioxide, Carbon Monoxide, Air, and Helium-Oxygen Mixtures," Proc. Phys. Soc. 85, 355 (1965).

3. L. M. Chanin, A. V. Phelps, and M. A. Biondi, "Measurements of the Attachment of Low Energy Electrons to Oxygen Molecules," Phys. Rev. 128, 219 (1962). This reference also indicates the variation of the coefficients with temperature.

4. A. N. Kontaratos, "On the Functional Dependence of Townsend's First Ionization Coefficient," Appl. Sci. Res. 12, 27 (1965).

5. Donald Arnush, P. J. Lynch, R. S. Margulies, and Paul Molmud, Current Status of the TRW High Altitude EMP Computer Program, TRW-11466-6053-T1-00, January 1969.

6. John Malik, private communication, January 1970.

7. H. J. Longley and C. L. Longmire, Development of the CHAP EMP Code, Mission Research Corporation Report Draft, MRC-R-3, January, 1972.

8. A. V. Phelps, private communication, Spring 1971.

9. C. E. Baum, Electron Thermalization and Mobility in Air, Air Force Weapons Laboratory, 16 July 1965 and AFWL EMP Theoretical Note 12, AFWL EMP 2-1, April 1971.

10. H. Hessenauer, "Anlagerung skoeffizienten and Driftgeschwindigkeiten von Elektronen in Luft," Zeitschrift für Physik 204, 142 (1967).

11. E. Kuffel, "Electron Attachment Coefficient in Oxygen, Dry Air, Humid Air and Water Vapor," Proc. Phys. Soc. 74, 297 (1959).

12. L. M. Chanin, A. V. Phelps, and M. A. Biondi, "Measurements of the Attachment of Low-Energy Electrons to Oxygen Molecules," Phys. Rev. 128, 219 (1962).

13. F. Biggs and D. E. Amos, Numerical Solutions of Integral Equations and Curve Fitting, Sandia Laboratories Research Report, SC-RR-71 0212, September 1971.

14. W. T. Wyatt, Jr., D. L. Jones, and D. H. Stump, NEPHI, An Electro-Magnetic Pulse FORTRAN Program User's Guide, U. S. Army Mobility Equipment Research and Development Center Report, Fort Belvoir, Virginia, December 1969.

15. Letter, J. S. Malik to Capt. C. S. Allen, 20 February 1970.